The influence of the electrolyte on the internal resistance of lithium-sulfur batteries studied by an intermittent current interruption method

Matthew J. Lacey*

Pre-print submitted to *ChemElectroChem*. Now published at doi: 10.1002/celc.201700129

1 Abstract

Galvanostatic cycling combined with an intermittent current interruption (ICI) resistance determination method is presented as a fast, accurate and comparatively simple method for following internal resistance changes in batteries over long term cycling. The technique is demonstrated here with a study of the influence of electrolyte composition and volume on the internal resistance of lithium-sulfur (Li-S) batteries. This approach is found to be particularly useful for the study of the Li-S system, where resistance changes considerably during charge and discharge as a result of compositional changes to the positive electrode and the electrolyte, but may also be valuable in the study of other battery systems.

2 Introduction

Determination of the internal resistance of a battery is valuable for a number of reasons. Foremost, it is a key performance indicator: voltage losses from ionic and electronic resistances in the materials and activation overpotentials of the cell reactions limit specific power and cause a loss of stored energy through Joule heating. Since resistance also tends to increase with usage, it is often an important indicator of a battery's state-of-health.

In the rechargeable lithium-sulfur (Li-S) battery system, for example, the considerable change in the chemical composition of both the electrode and electrolyte during operation [1–4] results in a significant variation of the internal resistance with the degree of charge (DoC) or discharge (DoD). As has been noted in the author's previous work [5] and by other authors, [2, 6–8] the internal resistance of a Li-S cell may vary by a factor of 2 or 3 or more with DoD.

*Department of Chemistry - Ångström Laboratory, Uppsala University, Box 538, Lägerhyddsvägen 1, 75 121 Uppsala, Sweden. email: matthew.lacey@kemi.uu.se

This characteristic is therefore important in the development of the Li-S system for applications such as electric vehicles (EV), for which it is of key interest due to the high practical gravimetric energy density of the system (> 300 Wh kg^{-1}). [9,10]

Furthermore, it is now well-established that the mechanism of the Li-S cell reaction is heavily dependent on many factors, particularly the electrolyte. [2,7, 11,12] The choice of solvent and salt influences the solubility and reactivity of intermediate polysulfide species, and the concentrations of these species in the electrolyte during operation will depend on the ratio of electrolyte to sulfur in the cell. The strong influence of the ratio of electrolyte to sulfur (often called the E/S ratio) on the cycling performance has been well-demonstrated elsewhere. [13–16] As the electrolyte is gradually destroyed by the negative electrode, it can be expected that the cycle life can be determined both by the amount of electrolyte and the susceptibility to decomposition of its components, as has also been demonstrated. [16,17] Clearly, the internal resistance of a Li-S cell can be expected to vary significantly not just with DoD/DoC, but with cycle number, and electrode and electrolyte composition. However, this is as yet relatively unexplored.

While there are a number of established electrochemical methods for determining internal resistance, the most commonly employed technique is electrochemical impedance spectroscopy (EIS), a powerful technique which allows for probing of the different contributing resistive and reactive processes in an electrochemical system across a wide range of timescales. However, its practical application is complicated because of the requirement for specialised equipment, and particularly the complexity in interpreting data, especially if validation by equivalent circuit modelling is desired. This complexity also renders analysis of a large number of measurements within a cycle over a large number of cycles highly time consuming, if not impractical. Very often, EIS is used for the purpose of comparison – for example, to determine if a system has a higher or lower overall impedance compared with an earlier state, or compared to a reference system. In such cases, a simpler method may suffice.

The aim of this work is to demonstrate the combination of a modified galvanostatic cycling program with short-duration intermittent current interruptions as an appropriate and simple method for continuously following internal resistance in batteries over extended cycling, with automated data analysis. By comparison with EIS, this approach is fast, comparatively accurate, can be made with available battery testing instruments and is simpler to interpret. This work constitutes a development of the work presented in a previous communication [5], in which this approach was applied to the study of Li-S cells containing Li metal negative electrodes of different thicknesses.

An overview of the technique along with a discussion of the improvements made in terms of accuracy is presented here. This method has been applied to a study of internal resistance in Li-S cells with relatively small changes in E/S ratio or composition relative to a well-established point of reference. The scope for future application of this technique will also be discussed.

3 Results and Discussion

3.1 The intermittent current interruption (ICI) method

In the previous communication [5], the use of an intermittent current interruption technique to follow the resistance changes in lithium-sulfur cells containing Li metal negative electrodes of different thicknesses was presented. A similar method has also been previously employed on a more limited basis for following the change in resistance with depth of discharge for $Li_4Ti_5O_{12}$-based electrodes [18].

However, in the previous reports, the voltage drop was determined by measuring the OCV at a single, fixed, time after the start of the current interruption (this is hereafter referred to as the single point method). Although this method is relatively simple from a data analysis perspective, the choice of any single fixed time is arbitrary, may be significantly influenced by C-rate, and may make comparison with measurements made by other techniques, or on other related systems, difficult.

A validation of the current interruption technique was presented as part of the Supporting Information of the earlier communication [5], in which the resistance of a Li-S cell was measured at the same state of charge (SoC) by both the "single point" method described above and compared with measurements made by EIS. The internal resistance was determined from the impedance spectra as the sum of the frequency-independent – "real" – resistances obtained from an equivalent circuit model; that is, the sum of all electronic and ionic resistances, contact resistances, charge transfer resistance, etc. The trend in resistance over 60 cycles was observed to be the same using both methods, but the current interrupt method in all cases gave higher estimations of the resistance than the EIS method. This overestimation occurs because the voltage drop includes contributions from reactive ("imaginary") processes such as diffusion, which can be accounted for in the equivalent circuit analysis of the impedance spectra.

From galvanostatic intermittent titration (GITT) measurements on both Li-S and Li-ion batteries it is typically observed that the cell voltage is linear with $t^{\frac{1}{2}}$ in a range of at least 0.1 – 10 s after a current interruption, across the entire state-of-charge window. The contribution of time-dependent processes on the timescale of the measurement can therefore be conveniently extrapolated out by regression to zero time after the interruption to obtain a better estimation of the sum of the "real" resistances. This approach is depicted in Figure 1. Note that the timescale of processes such as double layer charging is typically considerably shorter than 0.1 s, at least for the systems under consideration here.

This approach is validated by a recalculation of the same data presented in the Supporting Information of the previous work [5]. The recalculated data is given alongside the original measurements made by EIS and the single point method in Figure 2.

From Fig. 2 it is clear that the values obtained by the regression method are in good agreement with the EIS results, and considerably more so than the values from the previous "single point" method. This therefore demonstrates

that resistances determined by current interruption can be considered to be comparatively accurate and have a reasonable interpretation with respect to an equivalent circuit analysis of EIS measurements. Implementation of the method remains simple despite the more complex calculation of resistance here compared to the "single point" method. Data analysis is relatively straightforward using the "tidyverse" [19] add-on packages for the R programming language, and is fast: a typical dataset presented in this work with > 100 cycles of data with $> 10,000$ calculations of resistance can be processed automatically and – and visualised – in a matter of seconds on a modern personal computer.

3.2 ICI measurement of a Li–S battery

The electrolyte volume and composition selected as the baseline in this work is 6 μL mg_S^{-1} and 1 M LiTFSI, 0.25 M $LiNO_3$, 1:1 DME:DOL, as used in our previous publications. With this electrolyte system, the positive electrodes used in this work consistently deliver discharge capacities of the order of 900 mAh g_S^{-1} (2.3 – 2.8 mAh cm^{-2}) at 167.2 mA g_S^{-1} (approx. 0.42 – 0.5 mA cm^{-2}) for approximately 100 cycles. The time between resistance measurements of 5 min is equivalent to a capacity increment of 14 mAh g_S^{-1}, giving approximately 120 – 140 measurements of resistance per complete cycle.

A typical voltage profile for a single cycle of the above-described baseline system, with the associated internal resistance at each point, is given in Figure 3. Note the direction of charge and discharge as indicated by arrows. The observed changes in resistance on cycling are consistent with the previous communication [5] and with work published elsewhere. [2, 6] The measured resistances of less than 25 Ω cm^2 correspond to voltage drops of the order of 10 mV, at which level the assumption of Ohmic behaviour is reasonable. The principal feature is a more than doubling of the resistance during the discharge of the upper plateau; this increase is due to the dissolution of lithium polysulfides into the electrolyte, considerably increasing the viscosity of the electrolyte and reducing the ionic conductivity [6]. At an E/S ratio of 6 μL mg_S^{-1}, the dissolution of all sulfur in the electrode to form the polysulfide Li_2S_6 [3] without any precipitation of Li_2S implies an increase in the lithium ion concentration from 1.25 M to close to 3 M. A decrease in the ionic conductivity of the order of a factor of two is a reasonable expectation as a result of this concentration change. [2] Assuming all elemental sulfur is able to dissolve out of the positive electrode – that is, it is not rendered inactive by a lack of electrolyte access – an E/S ratio of 6 μL mg_S^{-1} is equal to 167 g_S L^{-1}, or a concentration of 5.2 M in S. This concentration is lower than at the congruent point in the phase diagram as determined for lithium polysulfides in DOL by Dibden *et al.* [20], so it is reasonable to assume that all sulfur exists in solution at this point. It has also been suggested that the increase may be related to charge transfer at the negative electrode [8]. However, this author has observed from preliminary three-electrode impedance measurements that the increase and decrease in resistance occurs is in the series resistance (i.e., at all frequencies), and that the charge transfer resistance of the negative does not change significantly.

Following this resistance peak, the resistance subsequently decreases, indicating a change in the electrolyte composition as polysulfides are converted to solid Li_2S and Li_2S_2 during the lower plateau. [3, 21] As discharge proceeds, a relatively small increase in the resistance is observed. This can also be understood as an expected result of the filling of pores and the passivation of the surface of the carbon host from the preciptitation of the discharge products; the increase of such a "precipitation resistance" has also been modelled by Zhang *et al.* [2] On charge, the resistance drops by a factor of two within the first $\sim 15\%$ of the charge, which can be understood as the release of conductive surface area and pore volume from the dissolution of the discharge products [1, 22]. The resistance increases and decreases again as the charge proceeds towards completion, indicating the reverse of the discharge reaction in the same state-of-charge window, however the change is smaller and broader than for the discharge reaction.

3.3 Effect of electrolyte volume

A series of cells containing a range of electrolyte volumes with E/S ratios of between 4 and 8 μL mg_S^{-1} were prepared and cycled under the same conditions as above until cell death. The discharge capacity and coulombic efficiency of the cells are plotted against cycle number in Figure 4; the resistance is plotted against capacity for selected cycles in Figure 5.

Fig. 4 shows the considerable dependence of cycle life on the E/S ratio. With 8 μL mg_S^{-1} cells were able to deliver reversible capacities of approximately 800 mAh g_S^{-1} after more than 180 cycles; with less than half of that amount, cells failed after less than 30 cycles. The results are comparable to those obtained by Thieme *et al.* [15] Coulombic efficiency for the largest electrolyte amount was approximately 97.5% for 70 cycles and gradually decreased thereafter. For all lower E/S ratios, the coulombic efficiency decreased gradually with cycling at a rate of about 1% every 10 cycles until cell failure. Cell failure is defined loosely here as a sudden increase in the resistance, a sudden drop in capacity, or other evidence of erratic cell behaviour.

As Fig. 5 shows, the resistance at the beginning of the test (the start of discharge on cycle 2; cycle 1 being the slow formation cycle) for all cells is approximately the same. The major peak in the resistance increases significantly as the electrolyte volume is reduced, rising from an initial value of 19 Ω cm^2 to a maximum of 107 Ω cm^2 for the smallest electrolyte volume. Cells with lower E/S ratios show higher resistances after the peak as discharge continues. These observations are consistent with the higher lithium polysulfide concentrations expected as a result of reducing the E/S ratio. It should be noted that at an E/S ratio of 4 μL mg_S^{-1}, the maximum possible sulfur concentration is 7.8 M in S, which may be in excess of the solubility of any of the polysulfide species. The changes in resistance are similar for all cells throughout the second charge, but the same trend towards higher resistances with decreasing electrolyte volume is observed.

As the cells are cycled, cell resistances gradually increase. In general, the

maximum resistance in the cycle, i.e., the major peak on discharge, is seen to increase with cycle number more quickly than the initial resistance, at the beginning of discharge. A plot of initial and maximum resistance against cycle number, and a separate plot of median resistance against cycle number, is given in the Supporting Information as Figures S1 and S2. For the cell with 4 μL mg_S^{-1} of electrolyte, the maximum resistance becomes so high after only five cycles that the discharge voltage cutoff of 1.8 V is reached at the end of the upper voltage plateau. The voltage profile for the fifth cycle of this cell, given in the Supporting Information as Figure S3, shows that the voltage at the end of the transition between the plateaus reaches close to 1.8 V but relaxes back to approximately 2.1 V before the end of discharge.

For low electrolyte volumes ($\sim 4-5$ μL mg_S^{-1}) especially, it is also clear from Fig. 5 that the resistance at all states of charge or discharge gradually increases with increasing cycle number. This and the above observations are consistent with the progressive decomposition of the electrolyte solvent and salt by the negative electrode. The increase in resistance independent of state-of-charge may be due to either a decrease in electrolyte conductivity or the deposition of insoluble products of solvent decomposition. In any event, these observations indicate that electrolyte decomposition is the principal cause of resistance increase and cell failure in these cells. This is also in agreement with the dependence of cycle life on electrolyte volume reported elsewhere. [16, 17]

It is also noted that in some cases, and only where the electrolyte volume is low, a resistance increase is also seen towards the very end of charge, coincident with the expected oxidation of polysulfides to elemental sulfur. This increase may also be understood to be a result of pore blocking and/or electrode passivation by solid sulfur, made more severe by the restricted electrolyte volume.

3.4 Effect of substitution of electrolyte salt

It has been recently reported that lithium polysulfides have a significantly lower solubility in DME:DOL-based electrolytes where lithium 4,5-dicyano-2-(trifluoromethyl)imidazolide (LiTDI) replaces LiTFSI as the electrolyte salt. [23] Because of this effect, and given the substantial dependence of the electrolyte volume on the cell resistance as discussed previously, it was expected that the substitution of LiTDI for LiTFSI should also significantly influence cell resistance. To investigate this, a series of cells were constructed with electrolytes containing LiTFSI, LiTDI and mixtures of LiTFSI and LiTDI in 2:1 and 1:2 molar ratios. The total amount of Li salt was fixed at 1.25 M (including 0.25 M $LiNO_3$) and the E/S ratio was also fixed at 6 μL mg_S^{-1}. The cells were tested under conditions identical to those used in the previous experiment. The coulombic efficiencies and discharge capacities against cycle number are plotted in Figure 6 and the resistance values against capacity, for selected cycles, are plotted in Figure 7.

Chen *et al.* [23] found that the substitution of LiTDI for LiTFSI improved coulombic efficiency and capacity retention in Li-S cells. However, it was found

here that the presence of LiTDI in the electrolyte was found to worsen cell performance in all cells where LiTDI was present. Fig. 6 shows that the rate of decrease in coulombic efficiency is larger with increasing LiTDI concentration, and is approximately double for the cell containing 1 M LiTDI compared to the LiTFSI reference over the first fifty cycles. The cells with the two highest concentrations of LiTDI showed sudden decreases in capacity after approximately 70 cycles - considerably earlier than cells containing with LiTFSI as the major salt. A probable cause is increased electrolyte decomposition in the cells where LiTDI was present. The reason for the disparity between these results and those of Chen *et al.* is not clear, but it should be noted that there are a number of differences in the materials and construction of the cell. However, the objective here is not to validate the findings of Chen *et al.*, and determining the reasons for the disparity is outside the scope of this work.

The cell resistance against capacity is presented for selected cycles in Fig. 7. For cycle 2 (that is, the first cycle after the initial formation cycle), it is clear that the initial resistance is almost identical for all electrolytes, as in the previous experiment. The major peak on the second cycle discharge is approximately twice as high for any LiTDI concentration compared to the LiTFSI reference. A trend towards higher peak resistances with higher LiTDI concentration is more clearly seen at the 10th discharge. Following Chen *et al.* and Dibden *et al.* [20] a solubility for long-chain polysulfides of the order of 1 M in S is expected, which would imply that precipitation of discharge products should take place before the peak, although there is no obvious difference in the voltage profiles between the cells (Supporting Information, Figure S4). A possible reason for the resistance increase is some passivation of the electrode surface, but this does not explain why the peak resistance is significantly higher than the resistance after the peak, which remains constant over the last 50% of discharge. The precipitation of Li_2S or other species in the pores of the host structure would appear not to significantly add to the internal resistance in the timescale studied here, at least until there is a significant degree of blocking of the pore volume and surface area. Alternative explanations are a more reduced ionic conductivity at higher concentrations for LiTDI-containing electrolytes, or slower reaction kinetics at this state-of-charge – perhaps as a result of the reduced solubility of polysulfides. Both are likely to contribute, however the measurement technique here can not distinguish between these effects. For the remainder of the second cycle discharge, the resistance remains roughly constant for all cells. By the 10th cycle, a new feature in the resistance profile can be seen. For the electrolyte with 1 M LiTDI and no LiTFSI, the resistance increases continuously over the last 50% of the discharge. The resistance at the end of discharge increases continuously with cycle number. A plot of every cycle between cycle numbers 2 and 15 is presented in the Supporting Information as Figure S5, which shows this resistance buildup. The same feature is ultimately seen in the cells with the mixed electrolyte systems. As discussed previously, this resistance increase could be understood as arising from the passivation of the electrode due to the insolubility of the discharge products. Since this behaviour was not seen in cells with low electrolyte volume in the previous experiment, nor was it seen

in the first few cycles in cells containing LiTDI, it does not seem reasonable to attribute this resistance increase to the effect of LiTDI on reducing polysulfide solubility. A possible explanation is that a decomposition product of LiTDI effects this resistance increase, and the continued decomposition of LiTDI causes this increase to become more severe with continued cycling. This hypothesis, of course, cannot be confirmed without a detailed analysis of the decomposition products formed in these electrolytes, but this may be an interesting topic for future research. Inspection of the 70th – 80th cycles (given in the Supporting Information as Figure S6) indicates that this resistance increase is responsible for the sudden capacity fade in this region. The same is true for the cell with the 1:2 TFSI:TDI electrolyte, although by the 70th cycle a general increase in resistance at all states of charge/discharge is apparent, likely indicating a general decomposition of the electrolyte and/or passivation of the electrode as seen in the previous experiment.

To summarise these measurements, the presence of LiTDI in the electrolyte clearly has a marked effect on the changes in the resistance of the cell on cycling. It is not obvious in this case that the differences in resistance can be correlated with the solubility of polysulfides alone. Differences in ionic conductivity and reaction kinetics may account for the differences in the resistance, and the results presented here suggest an effect related to the formation of decomposition products. However, these require further supporting experiments for confirmation.

3.5 Effect of changing DME:DOL ratio

The influence of varying the ratio of DME and DOL in the electrolyte system on the cell resistance was also investigated. The mixed DME:DOL solvent system is the most widely used in the current literature. [9] The reasons for the choice of solvents are well-established, and are a trade-off on the properties of each solvent. Polysulfide solubility is higher and reaction kinetics are faster in DME, but it reacts relatively quickly with the negative electrode; polysulfide solubility and kinetics are inferior in DOL, but DOL promotes the formation of a more stable surface layer on the negative electrode. [17] Consequently, a mixed solvent system is used for best overall performance, usually in a 1:1 DME:DOL ratio.

Cells were constructed with DME:DOL ratios of 3:1, 2:1, 1:1, 1:2, and 1:3, and cycled under the same conditions as for the previous experiments. The salt content was kept at 1 M LiTFSI and 0.25 M $LiNO_3$, and the E/S ratio was kept at 6 μL mg_S^{-1}. Coulombic efficiencies and discharge capacities plotted against cycle number are presented in in Figure 8, and resistances plotted against cycle number for selected cycles are presented in Figure 9.

Fig. 8 shows that the capacity and coulombic efficiency of the cells is very similar for all of the tested electrolyte systems over the first 100 cycles. It may be argued that the 2:1 and 1:1 DME:DOL compositions show the highest reversible capacities and coulombic efficiencies after 100 cycles and the electrolytes with higher DOL contents show worse performance, but the difference is relatively minor.

The resistance profiles, shown in Fig. 9, show much clearer differences between these cells. Over the first twenty cycles, a general trend can be seen in the major peak in resistance during discharge towards a higher resistance with larger DOL content, which similar to LiTDI-containing electrolytes may reflect relatively small differences in ionic conductivity and/or reaction kinetics. The resistance in the latter half of the discharge is also higher for the cells with higher DOL content, significantly so in the case of the 1:3 DME:DOL composition. This is consistent with an increased precipitation resistance [2] as a result of a lower solubility for polysulfides in DOL-rich electrolytes. The cells with the highest DME content show the lowest resistance throughout the duration of the experiment (this is also clearly shown on a plot of the median resistance against cycle number, given in the Supporting Information as Figure S7). It is also observed that a large increase in resistance is observed towards the end of charge in cells containing electrolytes with high DOL content. As observed in cells with reduced electrolyte volume, this increase is likely to be due to electrode passivation by precipitation of elemental sulfur, and further reflects a lower solubility for polysulfides.

4 Conclusions

It is demonstrated here that the ICI method is a convenient and valuable approach to following changes in resistance in batteries as a complement to standard methods such as galvanostatic cycling. The results presented herein constitute hundreds of thousands of measurements of resistance on 14 test cells, providing a level of information which is impractical to obtain by impedance spectroscopy. Each measurement is reduced to a single value, but one which has a physical relevance with respect to an equivalent circuit model of the system, namely the sum of all frequency-independent resistances. The assumption of an Ohmic voltage drop is reasonable for systems with low resistance cycled at low current densities; the influence of rate on the resistance determination has not been investigated here but errors may be expected at elevated rates.

The value of this technique to the study of the Li-S system is demonstrated in the results presented here. The variations in polysulfide solubility as a result of electrolyte volume, or salt or solvent selection, effect significant changes – sometimes up to an order of magnitude or more – in cell resistance as a function of state of charge. The changes in resistance reflect a variety of physical and chemical changes within the cell, such as passivation by insoluble products, changes in reaction kinetics due to formation of different species, and so on. While it must be noted that firm conclusions cannot be drawn from resistance measurements alone, the ability to correlate resistance changes with such processes, backed up by spectroscopic experiments, would surely be valuable in improving the understanding of the system. The technique is fully compatible with many *operando* techniques already in use.

In the systems investigated here, poorer cycle life was also correlated with higher cell resistances and increases in cell resistance. This technique may

therefore be valuable for evaluating cell stability as a complement or even an alternative to prolonged cell cycling. None of the alternative electrolyte compositions studied here gave improved performance compared to the baseline LiTFSI/$LiNO_3$/DME:DOL system.

It is also observed that the magnitude of cell resistance changes considerably depending on whether the cell is being charged or discharged, at least under constant current conditions. It is reasonable to assume that the resistance of a Li-S cell at any given time will depend on how the cell is being used; this has not been investigated here but is an interesting topic for future investigation.

A further possible extension to this technique is a three-electrode measurement using a reference electrode. Measuring the positive and negative electrode potentials simultaneously under the cycling conditions used in this work would allow for the determination of the resistances associated with each electrode, and how they change on cycling. Measurements of this type would be valuable in clarifying the processes contributing to resistance increase over time, and the implementation of such a three-electrode method will be pursued in future research. This approach is also expected to be valuable in the study of other battery systems, particularly those which show significant changes in resistance depending on the state of charge.

5 Experimental Section

5.1 Materials

Lithium bis(trifluoromethyl)sulfonimide (LiTFSI, Novolyte), lithium nitrate ($LiNO_3$, Aldrich) and lithium 4,5-dicyano-2-(trifluoromethyl)imidazolide (LiTDI) were dried at 120 °C under vacuum overnight prior to use. 1,3-dioxolane (DOL, anhydrous, Aldrich) was stored over 4 Å molecular sieves for at least 24 h prior to use. All other materials were used as received.

5.2 Electrode preparation

Sulfur powder (S, Aldrich) and Ketjenblack EC-600JD (KB, Akzo Nobel) were mixed manually in a 65:21 ratio and then heated to 155 °C for 20 minutes to melt sulfur into the pores of the carbon. The composite was then dispersed with conductive additives and binders into 5% EtOH in H_2O to give a final composition by weight of 65% S, 21% KB, 3.5% Super C65 (Imerys), 3.5% carbon nanofibers (CNF, 20 – 200 nm x 100 μm, Aldrich), 5.6% poly(ethylene oxide) (PEO, M_w ~4,000,000, Aldrich) and 1.4% poly(vinylpyrrolidone) (PVP, M_w 360,000). The slurry was mixed by planetary ball milling for 2 hours and cast onto graphite-coated Al foil (graphite loading ~ 0.02 mg cm^{-2}) by doctor blading to a loading of 2.5 – 3.0 mg_S cm^{-2}. The electrode coating was allowed to dry at ambient conditions, cut into 13 mm discs, dried further at 55°C under vacuum, and transferred to an Ar-filled glove box.

5.3 Cell preparation

CR2025 coin cells were assembled using the above-described positive electrodes, an Al_2O_3-coated porous polyethylene separator (MTI Corp.) and Li metal foil (125 μm thick, Cyprus Foote Mineral) as the negative electrode. The electrolyte was composed of 1 M Li salt (either LiTFSI or LiTDI, or a mixture thereof), 0.25 M $LiNO_3$ in a 1:1 mixture of 1,2-dimethoxyethane (DME, BASF) and DOL. The electrolyte amount was fixed relative to the mass of sulfur in the electrode and was varied between 4 and 8 μL mg_S^{-1} (total volume in the cell was between approximately 14 and 32 μL and was applied with a 10 μL adjustable autopipette). The water content of the electrolyte was determined to be < 25 ppm by Karl-Fischer titration.

5.4 Electrochemical testing

Electrochemical measurements were made using an Arbin BT-2043 battery testing system. All cells were rested at OCV for 6 hours and subjected to a formation cycle by discharging at 33.44 mA g_S^{-1} (C/50, based on the theoretical capacity of S) to 1.9 V and recharging at 66.88 mA g_S^{-1} (C/25) to 2.6 V. The cells were then cycled at a constant current of 167.2 mA g_S^{-1} (C/10, approx. 0.42 – 0.50 mA cm^{-2}) between voltage limits of 1.8 and 2.6 V. The current was interrupted (i.e., set to open circuit) every 5 min for 0.5 s. For each individual current interruption, the cell resistance was calculated assuming an Ohmic voltage drop (i.e., $R = dE/dI$). dE was calculated as the difference between $E_{I=0}$ – obtained by regression of E vs $t^{\frac{1}{2}}$ to zero time following the current interruption – and $E_{I\neq 0}$, measured immediately before the interruption. Data analysis and visualisation was performed using the R programming language and environment.

6 Acknowledgment

The Swedish Energy Agency are gratefully acknowledged for financial support. The Polymer Ionics Research Group is Warsaw University of Technology, Poland, is also gratefully acknowledged for providing the LiTDI used in this work.

7 Keywords

lithium, sulfur, battery, resistance, electrochemistry

8 TOC

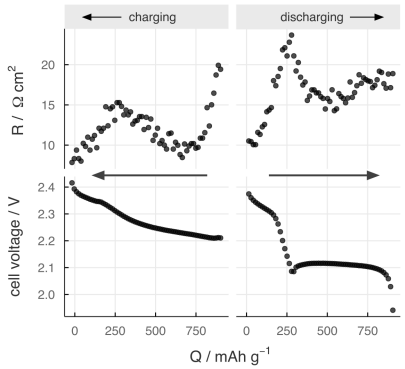

Always interrupting: Galvanostatic cycling combined with an intermittent current interruption (ICI) resistance determination method is presented as a fast, accurate and comparatively simple method for following resistance changes in batteries. The technique is applied here to a study of different electrolyte systems for the Li-S battery, where resistance changes considerably during charge and discharge as a result of compositional changes in the electrode and electrolyte.

References

[1] S. S. Zhang, *J. Power Sources* **2013**, 231, 153-162

[2] T. Zhang, M. Marinescu, L. O'Neill, M. Wild, G. Offer, *Phys. Chem. Chem. Phys.* **2015**, 17, 22581-22586

[3] M. Cuisinier, P.-E. Cabelguen, S. Evers, G. He, M. Kolbeck, A. Garsuch, T. Bolin, M. Balasubramaniam, L. F. Nazar, *J. Phys. Chem. Letts.* **2013**, 4, 3227-3232

[4] M. U. M. Patel, I. Arčon, G. Aquilanti, L. Stievano, G. Mali, R. Dominko, *ChemPhysChem* **2014**, 15 (5), 894-904

[5] M. J. Lacey, K. Edström, D. Brandell, *Chem. Commun.* **2015**, 51, 16502-16505

[6] V. Kolosnitsyn, E. Kuzmina, S. Mochalov, *J. Power Sources* **2014**, 252, 28-34

[7] C. Barchasz, J.-C. Leprêtre, F. Alloin, S. Patoux, *J. Power Sources* **2012**, 199, 322-330

[8] N. A. Cañas, K. Hirose, B. Pascucci, N. Wagner, K. Andreas Friedrich, R. Hiesgen, *Electrochimica Acta* **2013**, 97, 42-51

[9] M. Hagen, D. Hanselmann, K. Ahlbrecht, R. Maça, D. Gerber, J. Tübke, *Adv. Energy Mater.* **2015**, 1401986

[10] D. Eroglu, K. R. Zavadil, K. G. Gallagher, *J. Electrochem. Soc.* **2015**, 162 (6), A982-A990

[11] T. Pascal, K. H. Wujcik, D. R. Wang, N. P. Balsara, D. Prendergast, *Phys. Chem. Chem. Phys* **2017**, 19 (2), 1441-1448

[12] Y.-C. Lu, Q. He, H. A. Gasteiger, *J. Phys. Chem. C.* **2014**, 118, 5733-5741

[13] M. Hagen, P. Fanz, J. Tübke, *J. Power Sources* **2014**, 264, 30-34

[14] A. Jozwiuk, H. Sommer, J. Janek, T. Brezesinski, *J. Power Sources* **2015**, 296, 454-461

[15] S. Thieme, J. Brückner, A. Meier, I. Bauer, K. Gruber, J. Kaspar, A. Helmer, H. Althues, M. Schmuck, S. Kaskel, *J. Mater. Chem. A* **2015**, 3 (7), 3808-3820

[16] V. S. Kolosnitsyn, E. V. Kuzmina, A. L. Ivanov, *Russ. J. Electrochem.* **2016** 52, 273-282

[17] Y. V. Mikhaylik, I. Kovalev, R. Schock, K. Kumaresan, J. Xu, J. Affinito, *ECS Trans.* **2010**, 25, 23-34

[18] D. Wang, N. Ding, X. H. Song, C. H. Chen, *J. Mater. Sci.* **2009**, 44, 198-203

[19] http://www.tidyverse.org, H. Wickham, 2016.

[20] J. Dibden, J. Smith, N. Zhou, N. Garcia-Araez, J. R. Owen, *Chem. Commun.* **2016**, 52, 12885-12888

[21] S. Waluś, C. Barchasz, R. Bouchet, J.-C. Leprêtre, J.-F. Colin, J.-F. Martin, E. Elkaïm, C. Baehtz, F. Alloin, *Adv. Energy Mater.* **2015**, 5 (16), 1-5

[22] C.-S. Kim, A. Guerfi, P. Hovington, J. Trottier, C. Gagnon, F. Barray, A. Vijh, M. Armand, K. Zaghib, *J. Power Sources* **2013**, 241, 554-559

[23] J. Chen, K. S. Han, W. A. Henderson, K. C. Lau, M. Vijayakumar, T. Dzwiniel, H. Pan, L. A. Curtiss, J. Xiao, K. T. Mueller, Y. Shao, J. Liu, *Adv. Energy Mater.* **2016**, 6 (11), 1-6

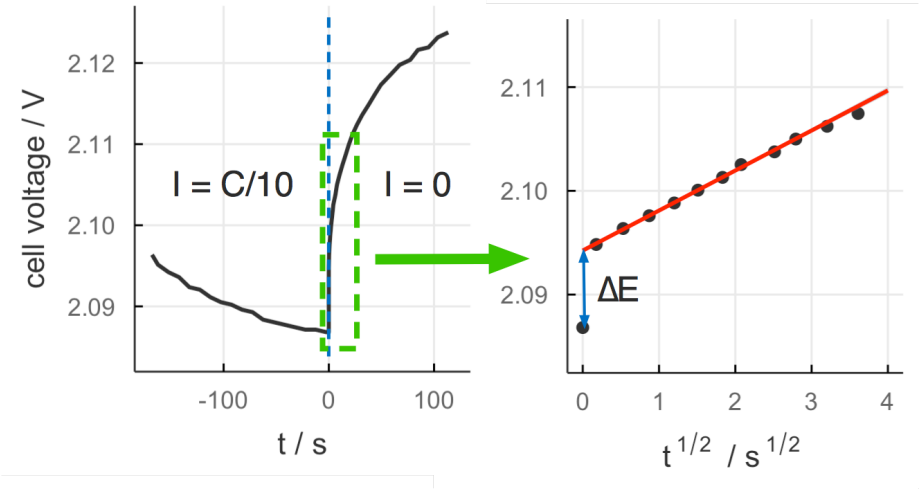

Figure 1: An example of a current interruption and regression of E vs $t^{\frac{1}{2}}$ used for calculation of internal resistance in a Li-S cell. In this work, only data points in the timescale $0.1 < t < 0.5$ s are used for the analysis.

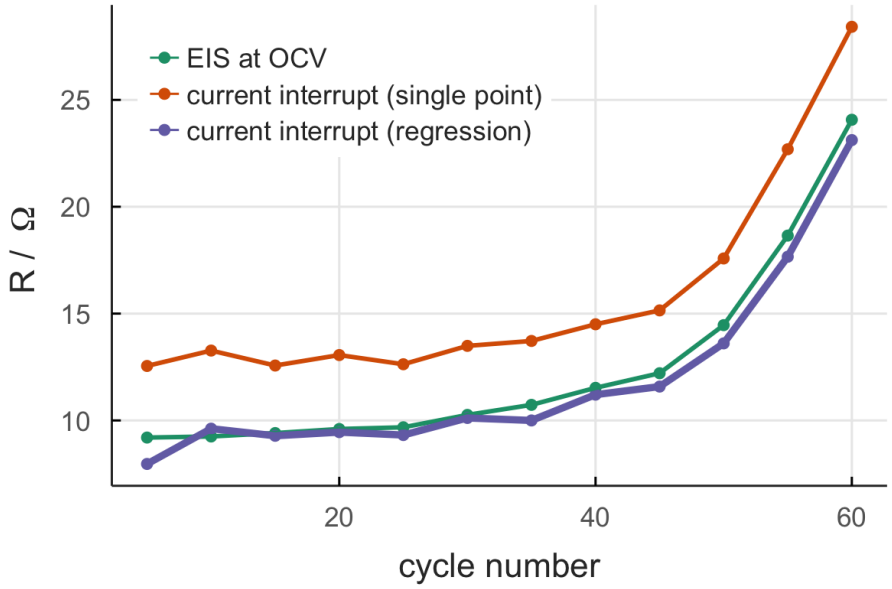

Figure 2: Internal resistance for a Li-S cell measured at approximately the same state of charge over 60 cycles measured by different techniques (data originally presented as Supporting Information in our previous work). The techniques used are: EIS at OCV following a 20-minute relaxation; measurement by current interruption using a single data point at a fixed time after the current interruption as in our previous study [5]; measurement by current interruption using the regression method described in this work.

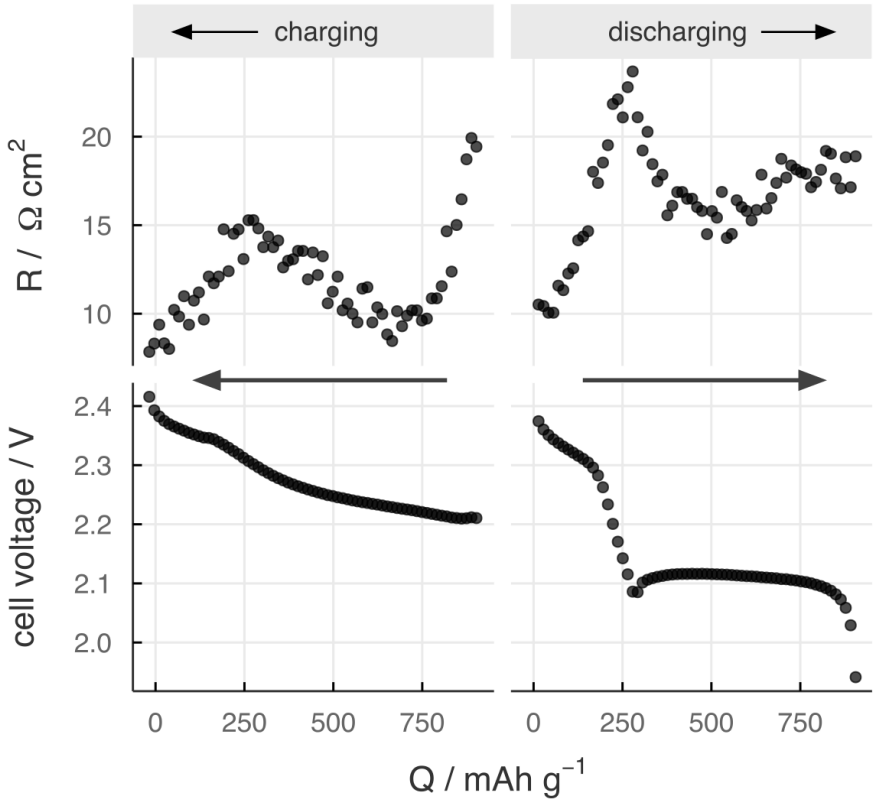

Figure 3: Cell voltage and internal resistance vs capacity for a single cycle of a Li-S cell using the specified "baseline" electrolyte composition and volume, at a current density of 167.2 mA g_S^{-1}. Arrows indicate direction of charge/discharge.

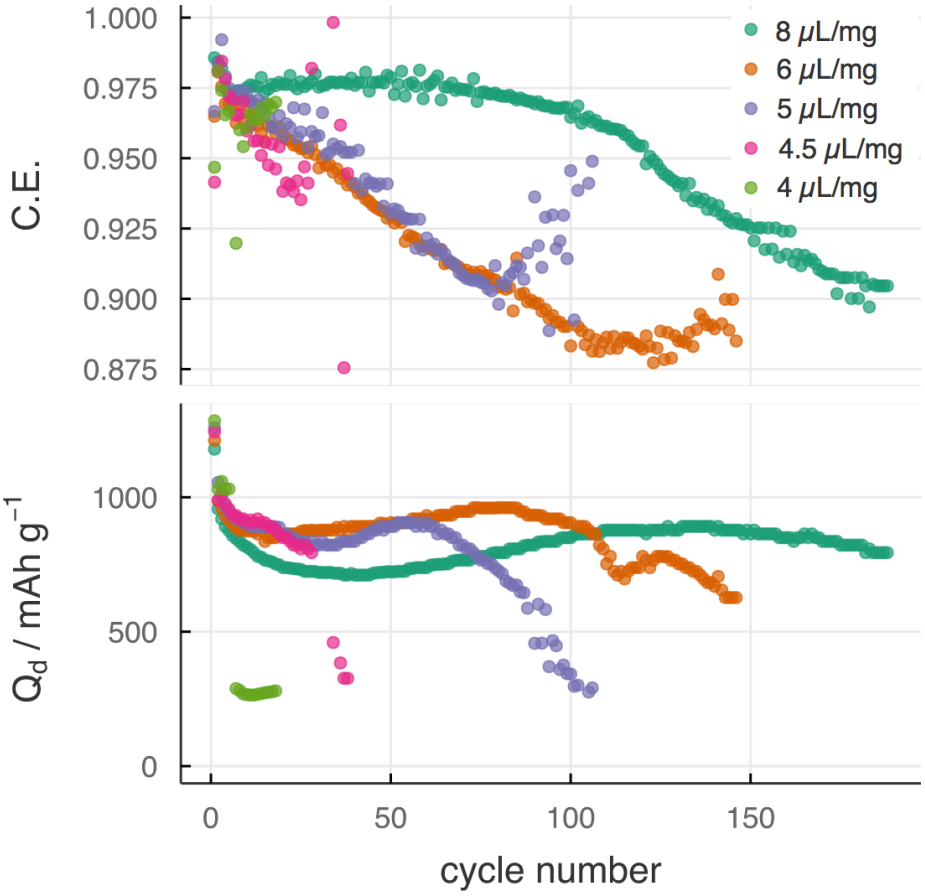

Figure 4: Coulombic efficiency and discharge capacity for Li-S cells containing different amounts of electrolyte, at a constant current density of 167.2 mA g_S^{-1}.

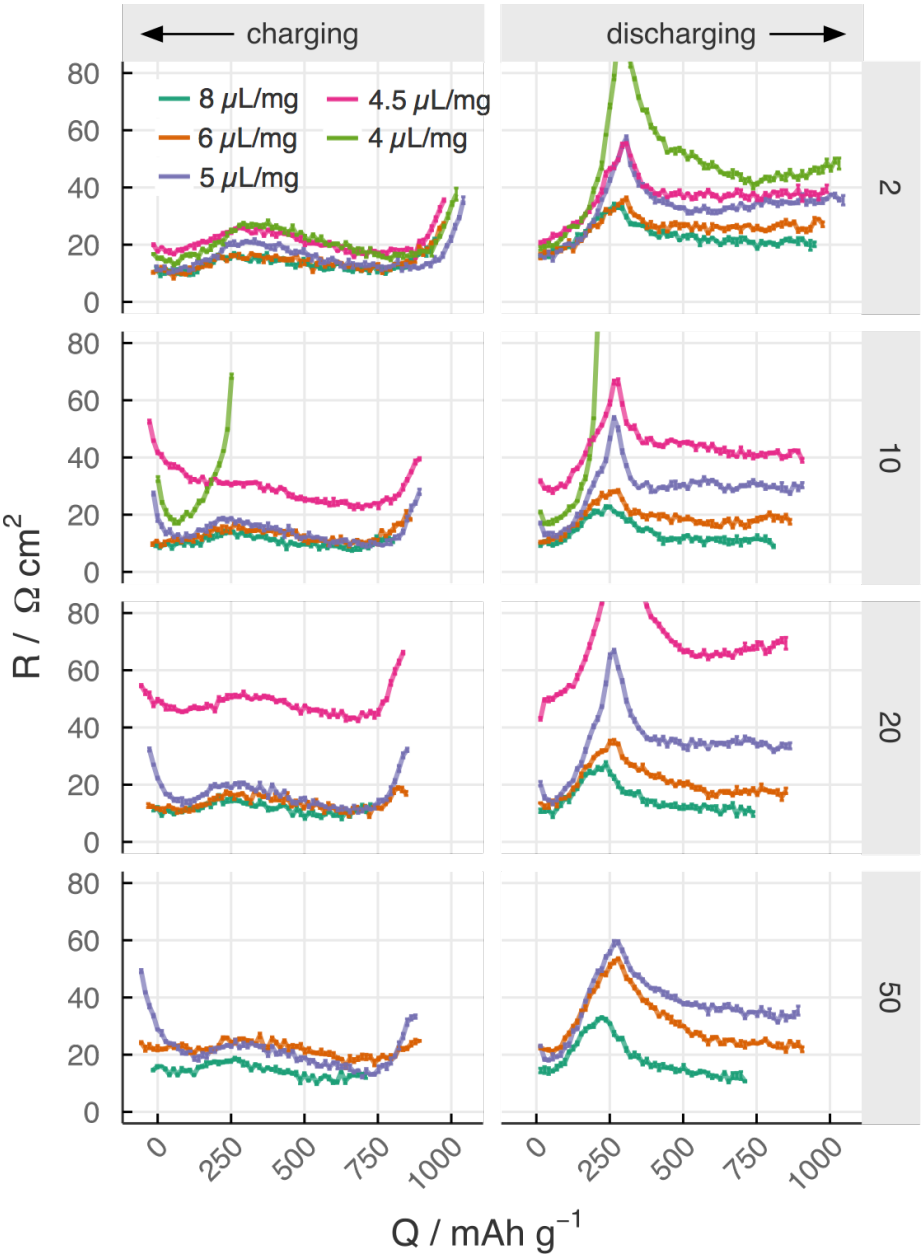

Figure 5: Resistance vs capacity for the Li-S cells described in Fig. 4 at the 2nd, 10th, 20th and 50th cycle (cycle number indicated by the strip on the right hand side of the plot.)

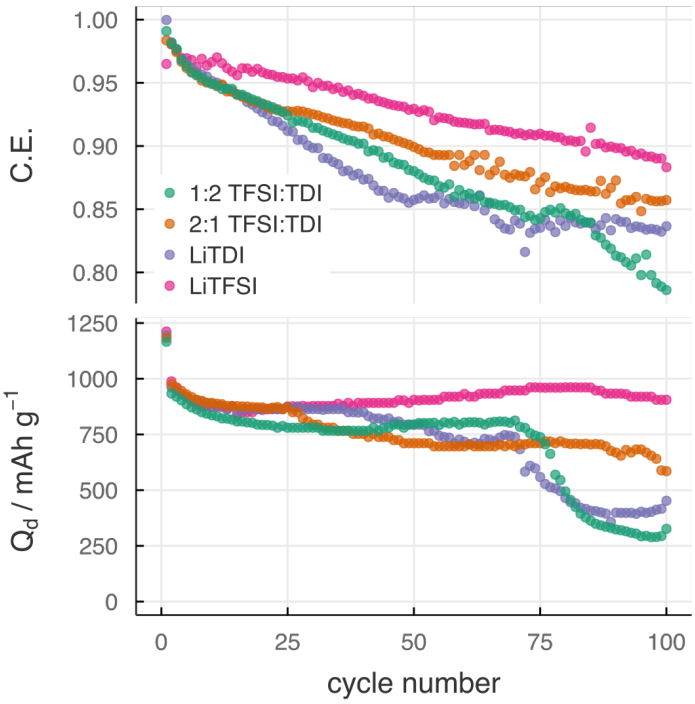

Figure 6: Coulombic efficiency and discharge capacity for Li-S cells containing different ratios of LiTFSI and LiTDI salt, at a constant current density of 167.2 mA g_S^{-1}. [LiTFSI] + [LiTDI] = 1 M for all cells.

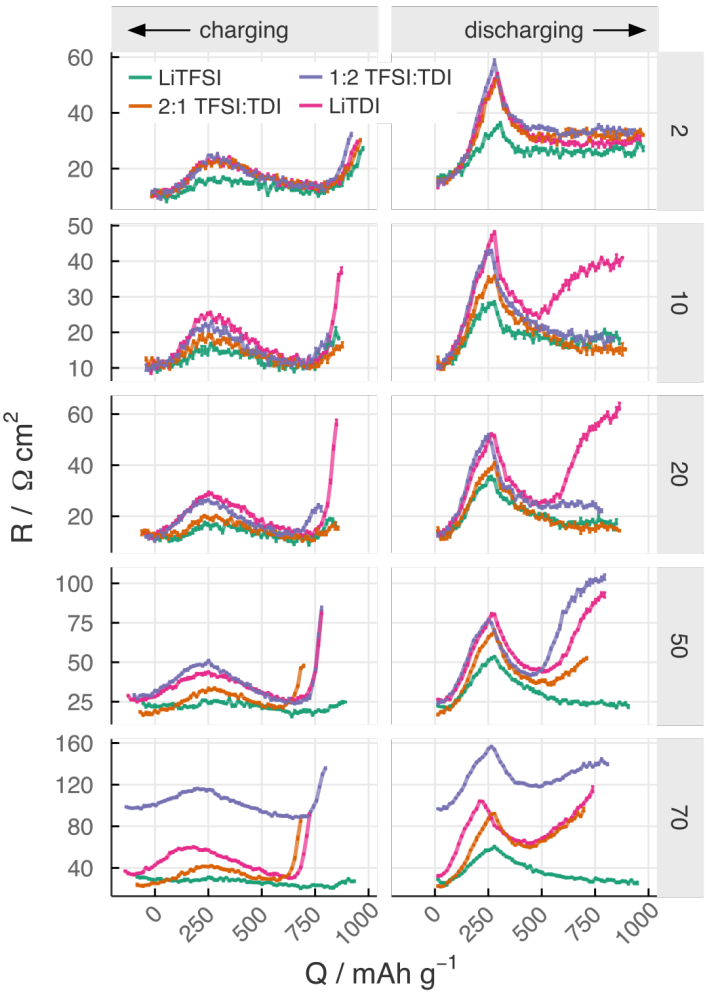

Figure 7: Resistance vs capacity for the Li-S cells described in Fig. 6 at the 2nd, 10th, 20th, 50th and 70th cycle (cycle number indicated by the strip on the right hand side of the plot.)

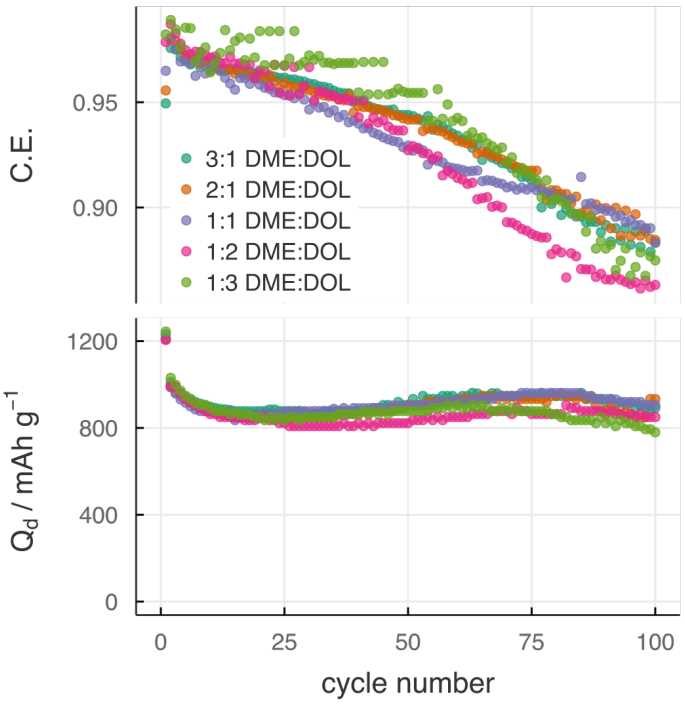

Figure 8: Coulombic efficiency and discharge capacity for Li-S cells containing electrolytes with DME and DOL solvents in different volume ratios, at a constant current density of 167.2 mA g_S^{-1}.

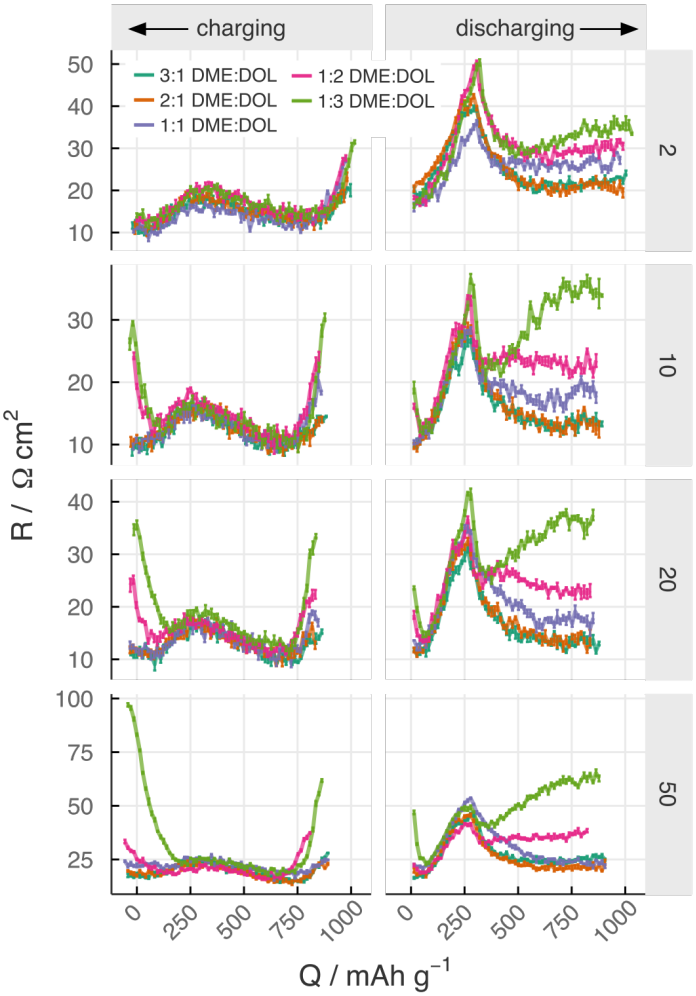

Figure 9: Resistance vs capacity for the Li-S cells described in Fig. 8 at the 2nd, 10th, 20th and 50th cycle (cycle number indicated by the strip on the right hand side of the plot.)